ELSEVIER

Journal of Alloys and Compounds 446–447 (2007) 237–241

Journal of ALLOYS AND COMPOUNDS

www.elsevier.com/locate/jallcom

Synthesis and dehydrogenation of $M(AlH_4)_2$ (M = Mg, Ca)

K. Komiya[a,*], N. Morisaku[a], Y. Shinzato[a], K. Ikeda[b], S. Orimo[b],
Y. Ohki[c], K. Tatsumi[c], H. Yukawa[a], M. Morinaga[a]

[a] *Department of Materials Science and Engineering, Graduate School of Engineering,*
Nagoya University, Chikusa-Ku, Nagoya 464-8603, Japan
[b] *Institute for Materials Research, Tohoku University, Sendai 980-8577, Japan*
[c] *Department of Chemistry, Graduated School of Science and Research Center for Materials Science,*
Nagoya University, Chikusa-Ku, Nagoya 464-8603, Japan

Received 28 September 2006; received in revised form 22 January 2007; accepted 23 January 2007

Abstract

$Mg(AlH_4)_2$ was synthesized by a metathesis reaction of $MgCl_2$ and $NaAlH_4$. It was decomposed in the two-step reactions, in agreement with the previous report [1]. The first reaction is characteristic of the decomposition to form MgH_2, and the second reaction is the further decomposition of this MgH_2 into some aluminum alloy phases. The decomposition temperature of the first reaction could be reduced remarkably when it was mixed with 1–5 mol% $TiCl_3$. For example, in the case of $Mg(AlH_4)_2$ mixed with 5 mol% $TiCl_3$ by ball-milling for 10.8 ks, a large portion of hydrogen was released during the milling at ambient temperature. The decomposition temperature of the first reaction decreased with increasing content of $TiCl_3$ in the specimen. However, the re-hydrogenation reaction scarcely occurred even in the pre-decomposed $TiCl_3$-containing specimen. For example, only 0.3 mass% of hydrogen was absorbed in the 1 mol% $TiCl_3$-doped specimen by exposing it for a long period to the hydrogen atmosphere of 30 MPa at 353 K. This result indicates that $Mg(AlH_4)_2$ is too unstable to progress the re-hydrogenation reaction smoothly. Therefore, $Ca(AlH_4)_2$ was chosen next, because this seems more stable than $Mg(AlH_4)_2$, judging from the phase stability diagram of complex hydrides proposed by us [2]. $Ca(AlH_4)_2$ was synthesized and its decomposition reactions were investigated in a fundamental manner.

Keywords: Complex hydride; Magnesium alanate; Hydrogen storage material; Catalyst

1. Introduction

Recently, complex hydrides such as $LiNH_2$ [3], $NaAlH_4$ [4] and $LiBH_4$ [5] have been investigated intensively because of their superiority in both the gravimetric and volumetric densities of hydrogen to conventional hydrogen storage alloys. However, for practical use of these complex hydrides, there are still several crucial problems such as the high decomposition temperature, poor irreversibility of hydrogenation and dehydrogenation reactions, and low reaction rates.

In view of chemical bonding, complex hydrides, $M(XH_m)_n$, are characterized by the covalent interaction between X and H ions to form a $[XH_m]^-$ ion and by the ionic interaction between M and $[XH_m]^-$ ions. On the basis of this understanding, a phase stability diagram of complex hydrides has been proposed using two parameters [2]. One is the bond energy of XH diatomic molecules and the other is the electronegativity difference, $\Delta\Phi_{X-M}$ between M and X ions. In the diagram unstable hydrides are located in the region of the low $\Delta\Phi_{X-M}$ and the low bond energy of XH, so they have a large possibility of releasing hydrogen at low temperatures.

The alanate-type complex hydrides have the lower $\Delta\Phi_{X-M}$ and the lower XH bond energy than the amide/imide-type hydrides such as $LiNH_2$ and $Mg(NH_2)_2$ [6], and the borohydride-type hydrides such as $LiBH_4$ and $NaBH_4$. In particular, $Mg(AlH_4)_2$ has the lowest $\Delta\Phi_{X-M}$ among the alanate-type hydrides. Therefore, it is expected that the phase stability of $Mg(AlH_4)_2$ will be low and hence it will release hydrogen more easily than the other complex hydrides. Recently, the crystal structure and the desorption process of $Mg(AlH_4)_2$ have been investigated [1,7–10].

---

[*] Corresponding author.
E-mail address: komiya@silky.numse.nagoya-u.ac.jp (K. Komiya).

0925-8388/$ – see front matter © 2007 Elsevier B.V. All rights reserved.
doi:10.1016/j.jallcom.2007.01.119

The purpose of this study is to investigate the dehydrogenation and re-hydrogenation reactions of $Mg(AlH_4)_2$ including the catalytic effects of $TiCl_3$. Furthermore, for comparison, $Ca(AlH_4)_2$ containing about 7.9 mass% H_2 was synthesized and its decomposition reactions were investigated in a fundamental manner.

2. Experimental

2.1. Synthesis of $Mg(AlH_4)_2$

$Mg(AlH_4)_2$ was synthesized by a metathesis reaction of $MgCl_2$ and $NaAlH_4$, in a diethylether (Et_2O) solution [7], and followed by purification and drying procedures. The reactions were expressed as

$$2NaAlH_4 + MgCl_2 \rightarrow 2NaCl + Mg(AlH_4)_2 \cdot Et_2O \quad \text{in diethylether } (Et_2O) \qquad (1)$$

$$Mg(AlH_4)_2 \cdot Et_2O \rightarrow Mg(AlH_4)_2 + Et_2O \qquad (2)$$

First, following the reaction (1), a mixture of $MgCl_2$ and $NaAlH_4$ with diethylether was heated and stirred under reflux at about 318 K for 2 days (86.4 ks). Then, using a Soxhlet apparatus, white crystalline $Mg(AlH_4)_2 \cdot Et_2O$ was extracted. Subsequently, following the reaction (2), the solvent, Et_2O, was removed from the product under vacuum, and fine white powders of $Mg(AlH_4)_2$ were obtained. Then, the temperature gradually increased from room temperature to 363 K to dry the powders.

2.2. Synthesis of $Ca(AlH_4)_2$

$Ca(AlH_4)_2$ was synthesized by a metathesis reaction of $CaCl_2$ and $NaAlH_4$, in a tetrahydrofuran (THF) solution, followed by purification. First, a mixture of $CaCl_2$ and $NaAlH_4$ with THF was heated and stirred under reflux at about 353 K for 1 day (43.2 ks). Then, the supernatant liquid of the mixture was decanted off using a syringe to separate by-product NaCl from $Ca(AlH_4)_2$, and THF solvent was dried off under vacuum. As a result, fine white powders of $Ca(AlH_4)_2 \cdot THF_x$ were obtained.

2.3. Analyses of $M(AlH_4)_2$ ($M = Mg$, Ca)

This final product was respectively examined using X-ray diffraction (XRD) with Ni-filtered Cu Kα radiation.

In addition, Raman spectroscopic analysis was performed with a 532 nm excitation laser at room temperature using a 600 grooves/mm grating, focused at 2200 cm^{-1}. The spectrum was measured in the range between 137 and 3822 cm^{-1}, with an accuracy of about 12 cm^{-1}. In a glove box, the specimen was set in a sealed holder prior to the measurement of Raman spectra.

Also, the final product was examined using thermal desorption mass spectroscopy (TDS) by increasing the temperature from 298 to 873 K at a constant heating rate of 5 or 0.5 K/min.

2.4. Synthesis of $TiCl_3$-doped $Mg(AlH_4)_2$ and its analyses

In addition, to promote the decomposition reaction, the final product was milled mechanically with X mol% $TiCl_3$ ($X = 1.0$, 1.5, 2.0 and 5.0). The milling was performed in a planetary ball mill apparatus (Firitsch P7) at 400 rpm for 3.6 ks under a hydrogen pressure of 1.5 MPa at ambient temperature. Then, the TDS measurements were carried out for all the specimens in the same way as used for pure $Mg(AlH_4)_2$. Also, the PCT measurements were conducted in the dehydrogenation reactions, using an ordinary Sieverts-type apparatus. Here, the measurements were recorded after 1.2 ks assuming equilibrium conditions were reached. Moreover, re-hydrogenation reactions were investigated by exposing the 1 mol% $TiCl_3$-doped specimen to the hydrogen atmosphere of 30 MPa at 353 K for a long time.

All the specimens were always handled in an argon-filled glove box equipped with a recirculation system to keep the water and oxygen concentrations below 1 ppm during operation.

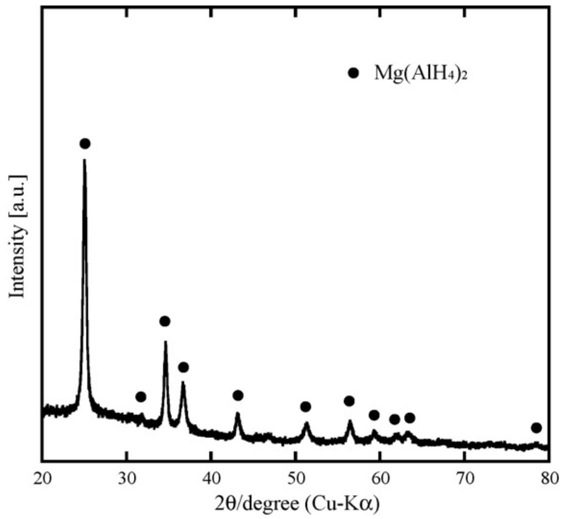

Fig. 1. X-ray diffraction profile of $Mg(AlH_4)_2$.

3. Results and discussion

3.1. Pure $Mg(AlH_4)_2$

The XRD profile of the final product is shown in Fig. 1. This result agreed with the report by Fichtner et al. [1]. Any peaks other than the magnesium alanate were not found, indicating that this specimen was composed of a single $Mg(AlH_4)_2$ phase.

The Raman spectrum was measured at room temperature. As shown in Fig. 2, it was characterized by the presence of the peaks around 1803 and 1966 cm^{-1} due to the Al–H stretching vibrational mode, and around 760–880 cm^{-1} due to the bending mode of Mg–H–Al molecules. This spectrum was also in good agreement with the one reported by Fichtner et al. [8]. The broad peaks around 3000 cm^{-1} arose from the impurities in the specimen, which is a residual organic material, the diethylether. The peaks were in good accordance with the reported IR spectrum of diethylether [11]. From these XRD and Raman spectrum

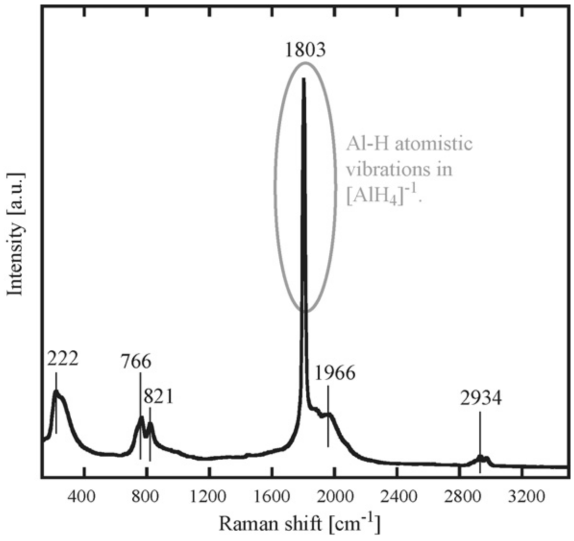

Fig. 2. Raman spectrum of $Mg(AlH_4)_2$.

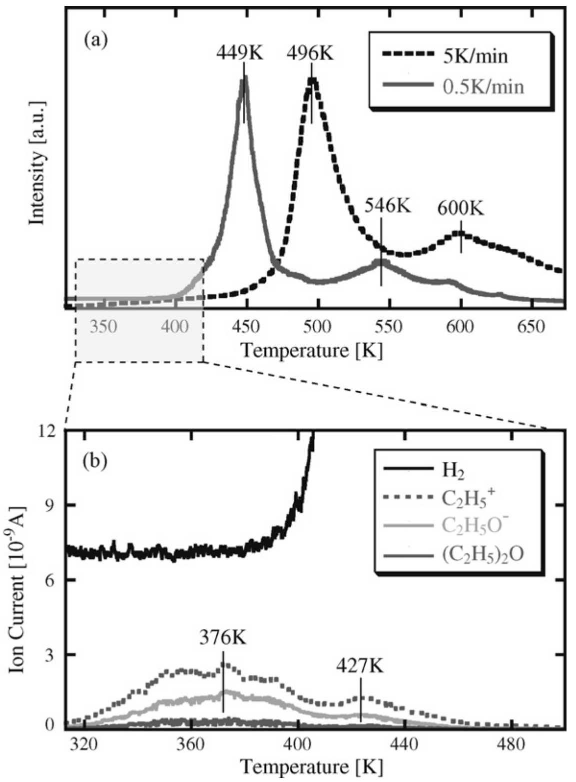

Fig. 3. TDS measurements of $Mg(AlH_4)_2$: (a) at different heating rates (5 and 0.5 K/min); (b) enlarged view of TDS peaks of H_2 and other fragment ions that are related diethyl ether (heating rate 0.5 K/min).

measurements, it was confirmed that pure $Mg(AlH_4)_2$ was synthesized successfully.

The thermal desorption curves for pure $Mg(AlH_4)_2$ are shown in Fig. 3(a). Here, the heating rates used were 5 and 0.5 K/min. As is evident from Fig. 3(a), $Mg(AlH_4)_2$ appeared to decompose in the two steps. The first and second steps occurred around 449 and 546 K in the case of the heating rate of 0.5 K/min, respectively. Following the recent experiment by Fossdal et al. [9], the first reaction probably corresponds to the reaction $(1 - x/2)Mg(AlH_4)_2 \rightarrow (1 - 3/2x)MgH_2 + 2\alpha(ss) + (3 + 3/2x)H_2$, whereas the second reaction corresponds to the reaction $(1 - 3/2x)MgH_2 + 2\alpha(ss) \rightarrow A\alpha + B\beta + (1 - 3/2x)H_2$. Here, α and β are the Al–Mg solid solution and some intermetallic phases, respectively [9]. The peak temperature for each reaction was reduced by about 50 K for both the reactions when the heating rate was changed from 5 to 0.5 K/min, since the kinetics of decompositon reaction depended on the heating rate.

In the case of the heating rate of 0.5 K/min, an enlarged illustration of the thermal desorption curves is shown in Fig. 3(b) for the emission of H_2 and other fragments of diethylether, such as $C_2H_5^+$, C_2H_5O and $(C_2H_5)_2O$. As a result, the amount of diethylether-like impurities remaining in the $Mg(AlH_4)_2$ specimen was found to be much lower than that of H_2, and the release of fragments was nearly completed at about 473 K.

3.2. $TiCl_3$-doped $Mg(AlH_4)_2$

The TDS experiments were carried out to investigate the catalytic effect of $TiCl_3$ on the decomposition temperature. The results of the TDS are shown in Fig. 4 for the $TiCl_3$-doped $Mg(AlH_4)_2$. It was apparent that the decomposition temperatures gradually decreased as the amount of $TiCl_3$ in the specimen increased from 1.0 to 2.5 mol%. The peak temperature for the hydrogen desorption was lowest in the 2.5 mol% $TiCl_3$-doped specimen among them. In the specimen doped with 5.0 mol% $TiCl_3$ by milling for 10.8 ks, most of the hydrogen in $Mg(AlH_4)_2$ appeared to be released during milling at ambient temperature, so that remarkable release of hydrogen was not observed as shown in Fig. 4(d). Also, a large increase in the pressure inside the milling pot was observed after milling.

The PCT curve of 1 mol% $TiCl_3$-doped $Mg(AlH_4)_2$ was measured in the dehydrogenation process at 333 K. As shown in Fig. 5, the total amount of hydrogen released from the specimen was about 3 mass%, and this value was much smaller than the theoretical one of about 7 mass% expected from the reaction $(1 - x/2)Mg(AlH_4)_2 \rightarrow (1 - 3/2x)MgH_2 + 2\alpha(ss) + (3 + 3/2x)H_2$ [9]. One possible reason is the kinetics of the decomposition of $Mg(AlH_4)_2$ was very slow even when a small amount of 1 mol% $TiCl_3$ was doped. The other possible reason is that a portion of hydrogen was released during milling at ambient temperature, so the PCT curve shown in Fig. 5 might not be

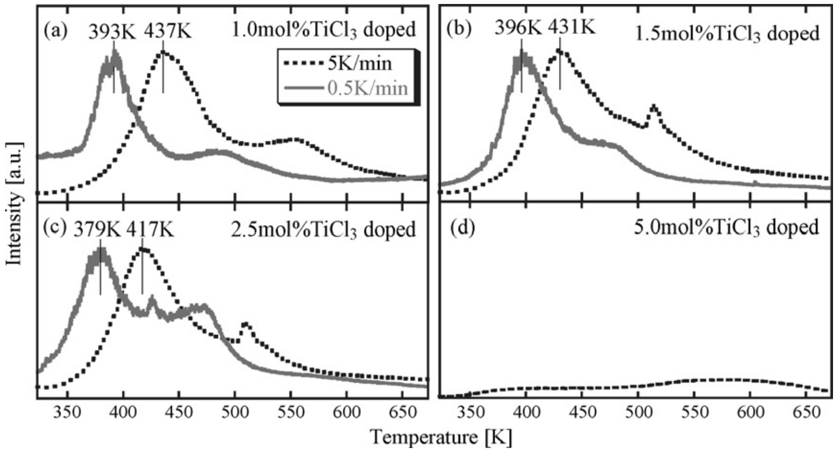

Fig. 4. TDS $TiCl_3$-doped $Mg(AlH_4)_2$, and $TiCl_3$ contents on: (a) 1.0 mol%; (b) 1.5 mol%; (c) 2.5 mol%; (d) 5.0 mol%.

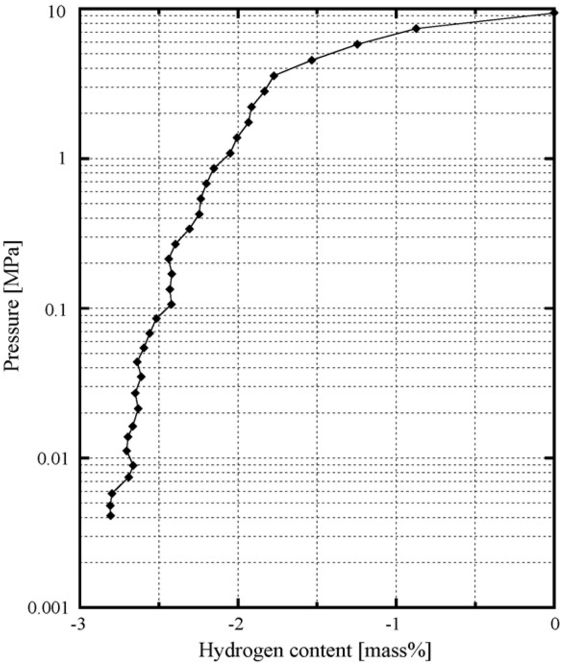

Fig. 5. PCT measurement of 1 mol% Ti-doped $Mg(AlH_4)_2$ at 333 K.

measured in the equilibrium condition. Judging from the PCT curve shown in Fig. 5, a plateau pressure of hydrogen will be higher than 10 MPa. This result indicates that $Mg(AlH_4)_2$ is a more unstable hydride than the other alanate hydrides such as $NaAlH_4$ and $KAlH_4$, in agreement with the prediction from the phase stability diagram [2].

The re-hydrogenation reactions were investigated for the 1 mol% $TiCl_3$-doped specimen by exposing it for a long time to the hydrogen atmosphere of 30 MPa at 353 K. Consequently, only 0.3 mass% of hydrogen was absorbed in the 1 mol% $TiCl_3$-doped specimen. This result indicates that $Mg(AlH_4)_2$ is too unstable so that the re-hydrogenation reaction can not take place smoothly in this condition. Therefore, it is important to make $Mg(AlH_4)_2$ more stable by alloying according to the phase stability diagram.

3.3. $Ca(AlH_4)_2 \cdot THF_x$

The XRD profile of the final product is shown in Fig. 6. New peaks different from that of $NaAlH_4$ or $CaCl_2$ or NaCl appeared. While the crystal structure of $Ca(AlH_4)_2$ was not revealed yet, this experimental profile was compared with the other reported one of $Ca(AlH_4)_2$ [12,13]. As a result, this profile was not in accordance with the other data because of the difference of the total amount of THF. According to SEM–EDX analysis, the content was determined to be 31 mol% Ca and 62 mol% Al, the value of which is close to the theoretical composition of $Ca(AlH_4)_2$.

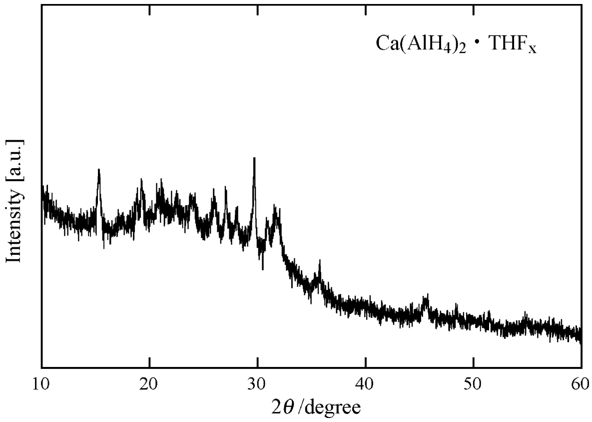

Fig. 6. XRD profile of $Ca(AlH_4)_2 \cdot THF_x$.

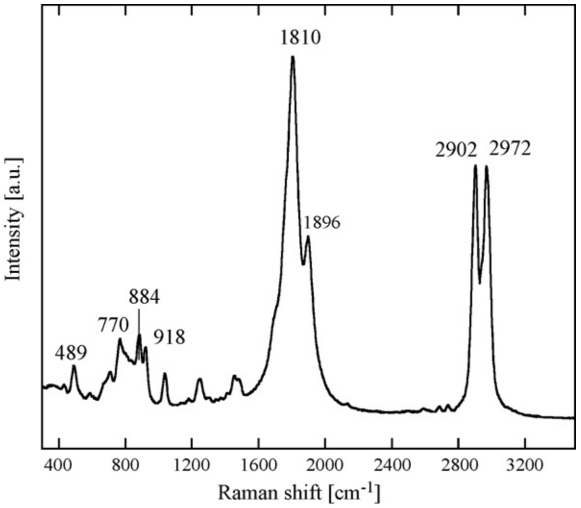

Fig. 7. Raman spectrum of $Ca(AlH_4)_2 \cdot THF_x$.

The Raman spectrum measured at room temperature is shown in Fig. 7. It was characterized by the presence of strong peaks at 1810 and 1896 cm^{-1} due to the Al–H stretching vibrational mode, and around 770–918 cm^{-1} due to the bending mode of Ca–H–Al molecules. The sharp peaks around 3000 cm^{-1} come from a residual organic material, THF, whose peaks were in accordance with the reported IR spectrum of THF [11]. From these XRD, SEM–EDX and Raman measurements, it was thought that $Ca(AlH_4)_2 \cdot THF_x$ was synthesized.

The thermal desorption curves are shown in Fig. 8 for $Ca(AlH_4)_2 \cdot THF_x$. Here, the heating rate used was 0.5 K/min.

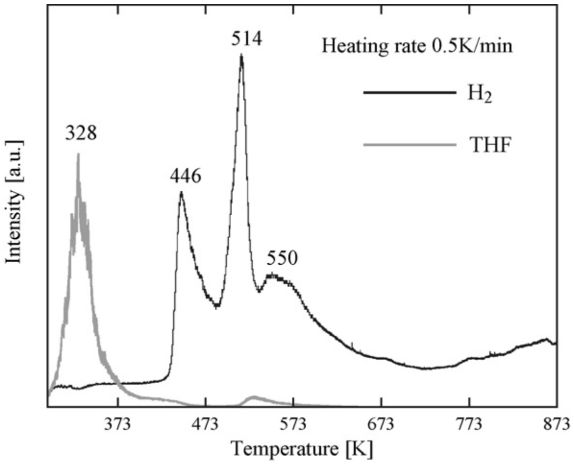

Fig. 8. TDS measurement of $Ca(AlH_4)_2 \cdot THF_x$.

As is evident from Fig. 8, $Ca(AlH_4)_2 \cdot THF_x$ appeared to decompose in the three steps. The first, second and third steps occurred around 446, 514 and 550 K, respectively. However, each dehydrogenation reaction was not revealed yet. Compared with the results of $Mg(AlH_4)_2$ shown in Fig. 3(a), it was found that $Ca(AlH_4)_2 \cdot THF_x$ is more stable than $Mg(AlH_4)_2$. Further experiments are now under way.

4. Summary

$Mg(AlH_4)_2$ was synthesized by a metathesis reaction of $MgCl_2$ and $NaAlH_4$. According to the thermal desorption analysis, $Mg(AlH_4)_2$ was decomposed in the two steps. The first reaction is characteristic of the decomposition to form MgH_2, and the second reaction is the further decomposition of this MgH_2 into some aluminum alloy phases. However, in the case of $Mg(AlH_4)_2$ doped with 1–5 mol% $TiCl_3$ by ball-milling, the onset temperatures of the first and second steps was reduced significantly. For $Mg(AlH_4)_2$ doped with 5 mol% $TiCl_3$ by ball-milling for 10.8 ks, most of hydrogen was released during milling at ambient temperature. Also, for $Mg(AlH_4)_2$ doped with 1 mol% $TiCl_3$, about 3.0 mass% of hydrogen was released at 333 K.

According to the PCT measurement, a plateau pressure of hydrogen was expected to be higher than 10 MPa. However, the re-hydrogenation reaction scarcely occurred even in the pre-decomposed $TiCl_3$-containing specimen. This means that $Mg(AlH_4)_2$ is a more unstable hydride, as compared to the other alanate hydrides such as $NaAlH_4$ and $KAlH_4$. Therefore, it is important to make $Mg(AlH_4)_2$ more stable to some extent by alloying. For comparison, $Ca(AlH_4)_2$ was synthesized and its decomposition reactions were investigated in a fundamental manner. As a result, $Ca(AlH_4)_2$ was found to be more stable than $Mg(AlH_4)_2$.

Acknowledgments

This study was supported by a Grant-Aid for Science Research from the Ministry of Education, Culture, Sports, Science and Technology of Japan, by the Japan Society for the Promotion of Science, and also by the 21st Century COE Program, “Nature-Guided Materials Processing” in Nagoya University.

References

[1] M. Fichtner, O. Fuhr, O. Kircher, J. Alloys Compd. 356–357 (2003) 418–422.
[2] M. Yoshino, K. Komiya, Y. Takahashi, Y. Shinzato, H. Yukawa, M. Morinaga, J. Alloys Compd. 404–406 (2005) 185–190.
[3] T. Ichikawa, S. Isobe, N. Hanada, H. Fujii, J. Alloys Compd. 365 (2004) 271–276.
[4] B. Bogdanović, R.A. Brand, A. Marjanović, M. Schwickardi, J. Tölle, J. Alloys Compd. 302 (2000) 36–58.
[5] A. Züttel, P. Wenger, S. Rentsch, P. Sudan, Ph. Mauron, Ch. Emmenegger, J. Power Sources 118 (2003) 1–7.
[6] Y. Nakamori, G. Kitahara, K. Miwa, S. Towata, S. Orimo, Appl. Phys. A 80 (2005) 1–3.
[7] M. Fichtner, O. Fuhr, J. Alloys Compd. 345 (2003) 286–296.
[8] M. Fichtner, J. Engel, O. Fuhr, O. Kircher, O. Rubner, Mater. Sci. Eng. B 108 (2004) 42–47.
[9] A. Fossdal, H.W. Brinks, M. Fichtner, B.C. Hauback, J. Alloys Compd. 404–406 (2005) 752–756.
[10] Y. Kim, E. Lee, J. Shim, Y.W. Cho, K.B. Yoon, J. Alloys Compd. 422 (2006) 283–287.
[11] http://www.ansyco.de/IR-Spektren/index2.html?Diethylether.html~Liste-D.html.
[12] M. Fichtner, C. Frommen, O. Fuhr, Inorg. Chem. 44 (2005) 3479–3484.
[13] M. Mamatha, B. Bogdanović, M. Felderhoff, A. Pommerin, W. Schmidt, F. Schüth, C. Weidenthaler, J. Alloys Compd. 407 (2006) 78–86.